energies

MDPI

Article

Adsorption Equilibria and Systematic Thermodynamics Analysis of Carbon Dioxide Sequestration on South African Coals Using Nonlinear Three-Parameter Models: Sips, Tóth, and Dubinin–Astakhov

Major Melusi Mabuza [1,*] and Mandlenkosi George Robert Mahlobo [2]

[1] Department of Chemical Engineering Technology, Faculty of Engineering and the Built Environment, University of Johannesburg, P.O. Box 17011, Doornfontein, Johannesburg 2088, South Africa
[2] Department of Chemical and Materials Engineering, University of South Africa, P.O. Box 392, Roodepoort 1709, South Africa; mahlomg@unisa.ac.za
* Correspondence: majorm@uj.ac.za

Abstract: Carbon dioxide (CO_2) injection into geologic formations has gained global traction, including in South Africa, to mitigate anthropogenic emissions through carbon capture, utilisation, and storage technology. These technological and technical developments require a comprehensive and reliable study of CO_2 sorption equilibria under in situ unmineable coal reservoir conditions. This paper presents novel findings on the study of the equilibrium adsorption of CO_2 on two South African coals measured at four temperatures between 30 and 60 °C and pressures up to 9.0 MPa using the volumetric technique. Additionally, the sorption mechanism and thermodynamic nature of the process were studied by fitting the experimental data into Langmuir–Freundlich (Sips), Tóth, and Dubinin–Astakhov (DA) isotherm models, and the Clausius–Clapeyron equation. The findings indicate that the sorption process is highly exothermic, as presented by a negative temperature effect, with the maximum working capacity estimated to range between 3.46 and 4.16 mmol/g, which is also rank- and maceral composition-dependent, with high-rank vitrinite-rich coal yielding more sorption capacity than low-rank inertinite-rich coal. The experimental data fit well in Sips and Tóth models, confirming their applicability in describing the CO_2 sorption behaviour of the coals under the considered conditions. The isosteric heat of adsorption varied from 7.518 to 37.408 kJ/mol for adsorbate loading ranging from 0.4 to 3.6 mmol/g. Overall, the coals studied demonstrate well-developed sorption properties that characteristically make them viable candidates for CO_2 sequestration applications for environmental sustainability.

Keywords: anthropogenic emissions; CO_2 sequestration; isotherm models; sorption equilibria; thermodynamics; unmineable coal

check for updates

Academic Editor: Dameng Liu

Received: 27 March 2025
Revised: 9 May 2025
Accepted: 19 May 2025
Published: 20 May 2025

Citation: Mabuza, M.M.; Mahlobo, M.G.R. Adsorption Equilibria and Systematic Thermodynamics Analysis of Carbon Dioxide Sequestration on South African Coals Using Nonlinear Three-Parameter Models: Sips, Tóth, and Dubinin–Astakhov. *Energies* **2025**, *18*, 2646. https://doi.org/10.3390/en18102646

Copyright: © 2025 by the authors. Licensee MDPI, Basel, Switzerland. This article is an open access article distributed under the terms and conditions of the Creative Commons Attribution (CC BY) license (https://creativecommons.org/licenses/by/4.0/).

1. Introduction

The continued reliance of industrialisation on a fossil fuel-dominated energy mix has greatly contributed to the problem of greenhouse gas emissions, particularly in the last three decades. The anthropogenic emissions of carbon dioxide (CO_2), methane (CH_4), and nitrous oxide (N_2O) have been the main contributors to global warming [1]. Over 38 billion tonnes of CO_2 are released into the atmosphere per annum, of which 45% is from coal, 35% from oil, and 20% from gas [2,3]. The Intergovernmental Panel on Climate Change [4] has recently warned that, at this rate, the surface temperature will increase

by 1.5 °C above the pre-industrialisation (1850–1900) levels within the first half of the 2030s, and this would make it challenging to maintain the temperature increase by 2.0 °C later in the 21st century. Consequently, these increments will intensify the multiple and concurrent natural disasters, like floods, droughts, heat waves, and cyclones [3], that impede the United Nations' efforts on climate action (Sustainable Development Goal-13) and the eradication of poverty (Sustainable Development Goal-1).

Reducing CO_2 emissions is a primary and urgent solution to be achieved through the establishment and implementation of new technologies, including the carbon capture, utilisation, and storage (CCUS) [5]. CCUS has been identified as a modern alternative for CO_2 removal, which involves geological sequestration of CO_2 in unmineable coal seams, basaltic formations, depleted oil and gas reservoirs, deep saline aquifers, and the ocean [5,6]. Also, South Africa, through the integrated resource plan (IRP) of the Department of Mineral Resources and Energy, recognises CCUS technology as one of the key role players in the energy mix and clean coal technology [7,8]. Although there are already over 40 large-scale integrated CCUS facilities globally [9], Chen et al. [10] asserts that the years 2040 to 2060 will mark the "Golden Age" of CCUS deployment.

Of the geological storage options that are currently being explored, carbon dioxide sequestration in deep unmineable coal seams has been projected to provide the essential geological storage volume globally [11,12], since coal comprises a complex porous network of organic and inorganic matter with varying surface functionalities that enables it to have a high affinity for favourably adsorbing CO_2 molecules [13,14]. The South African Council for Geoscience (CGS) identified 1.386 gigatons of CO_2 storage potential to be available in unmineable coal seams [15], with the majority being close to the CO_2 emissions source points (i.e., Sasol and Eskom power stations). However, there has been little to no comprehensive CO_2 storage capacity evaluation conducted on these coal seams, including the assessment of the theoretical, effective, practical, and matched CO_2 uptake, as well as the thermodynamic studies and theoretical modelling. Only a few studies [16–19] have been conducted based on CO_2 uptake in these deep unmineable coal seams at high pressure and temperature. Most of the studies focused on the theoretical CO_2 sorption capacity from low pressure to supercritical pressure and evaluated the physicochemical coal properties in relation to CO_2 sorption [20–22], with no thermodynamics and theoretical modelling of the sorption process conducted.

Determining the gas sorption properties of a particular coal is significant to assess the gas saturation and long-term stability in a coalbed. This is determined experimentally by measuring the gas sorption capacity under various in-seam environmental conditions (moisture, temperature, pressure, and pH) [23,24]. The nature of the coal determines its maximum possible sorption capacity. However, the extent to which that capacity may be realised depends on the dynamic character of the sequestration environment [25]. Therefore, the surface characteristics and molecular compatibility of coal are demonstrated by equilibrium studies, which estimate the coalbed's potential to store CO_2 through sorption under isothermal conditions. Based on the South African context, early studies on CO_2 equilibrium were investigated by Bhebhe [26] on coals acquired from Waterberg, Witbank, and KwaZulu–Natal coalfields in South Africa. The experimental measurements were conducted at a temperature of 30 °C and a maximum pressure of 0.150 MPa, and they reported sorption capacities ranging from 0.072 to 3.236 mmol CO_2 per g of coal. A study by Gertenbach [27] focused on single-component CO_2 and methane (CH_4) sorption studies on coal samples from the South African Waterberg and Highveld coalfields at 22 °C and 5.0 MPa, and yielded CO_2 sorption capacities ranging between 1.26 and 2.84 mmol/g. Similar studies were conducted by Maphala and Wagner [18], as well as Okolo et al. [16] under subcritical to supercritical conditions, and they reported CO_2 sorption capacities of

2.8–5.0 mmol/g and 0.925–1.377 mmol/g, respectively, with the vitrinite-rich coals having a stronger CO_2–coal interaction due to the dominance of microporous regions [28].

The modelling of the sorption behaviour and thermodynamic properties gives insight into the interaction between the coal matrix and CO_2 based on the assumptions stipulated by each model [24,29]. The modelling, interpretation, and understanding of adsorption isotherm data modelling has developed into a valuable and crucial technique for predicting the performance of the adsorption system, which is necessary for comprehending the adsorption mechanism and adsorption system design. The distribution of adsorbates may be quantified using the regression analysis approach, which evaluates the adsorption system and confirms the coherence of the theoretical assumptions of the adsorption isotherm model, making it one of the most often used tools for identifying the best-fitting adsorption models [30]. Up to now, many researchers have continued to heavily rely on linear regression analysis using two-parameter isotherm models for gas–solid systems [31–33]. The non-linear regression analysis using three-parameter sorption isotherm models is more effective than the linearised two-parameter models, since it significantly reduces the error between the theoretical isotherm and the experimental data [34], considers the amount of gas adsorbed on both the fixed and unoccupied sites as a monolayer on the adsorbent matrix, and accounts for the density ratio of the "free" phase and the sorbed phase [35]. Therefore, continuous knowledge development of geological formations will expedite a deep understanding of CO_2–coal interactions during storage for safer and more reliable design systems that prolong CO_2 storage and minimise any environmental impacts and concerns [36].

The three-parameter isotherm models, Sips, Tóth, and Dubinin–Astakhov, are used for modelling sorption data for single-component gases under isothermal conditions [37]. The non-linear curve produced by the modelled experimental adsorption isotherm represents the adsorption process, and the mathematical correlation examined in the modelling study provides crucial information for the adsorption system's operational design and real-world application [38]. The thermodynamic property, namely the isosteric heat/enthalpy of adsorption, which is the heat released when an adsorptive binds to an adsorbent surface [39], is often evaluated together with the modelling of the experimental data, since it also describes the interactions between the adsorbate and the adsorbent. The curve generated by the plot of the amount of adsorbate adsorbed vs. the differential enthalpies of adsorption provides information related to the surface coverage energetics and micropore filling [29]. Higher magnitudes (i.e., more negative) of the isosteric enthalpy of adsorption ($\Delta H_{ads} < 0$ kJ/mol) for a given gas–solid system suggests that there will be more gas adsorbed at a given temperature and pressure, which suggests that there are no activation barriers and the process is physisorption. The opposite is chemisorption, which is characterised by chemical interactions and bonds with higher activation energies, like most chemical reactions [39].

When viewing the context of traditional theoretical adsorption isotherm models related to coal heterogeneous surface coverage and microporous filling, it comes as no surprise that there is a knowledge shortfall in the literature in understanding the practical implications of model parameters in the actual adsorptive system design. Therefore, this work intends not only to discuss the theoretical methodologies but also to formulate a clear correlation between adsorbent–adsorbate interaction and the adsorption system design by comprehensively interpreting the model parameters for other researchers to consider with data from CO_2 adsorption isotherms. Therefore, this paper is part of a comprehensive study of CO_2 sequestration into South African unmineable coalfields. The paper aims to present the CO_2 sorption equilibrium data of South African coal, with a rank classification of anthracite (vitrinite-rich) and bituminous (inertinite-rich). The sorption studies

were evaluated under supercritical conditions (temperatures ranging from 30–60 °C and pressures up to 9.0 MPa) using non-linear three-parameter adsorption isotherm models (Dubinin–Astakhov, Langmuir–Freundlich (Sips), and Tóth) regressions and thermodynamic properties (isosteric heat/enthalpy of adsorption) to create an expanded fundamental understanding and predict the CO_2 sorption behaviour and characteristics of these South African coal matrices and the adsorption system design to maximise long-term CO_2 storage and minimise any environmental and safety concerns.

2. Materials and Methods

2.1. Materials

The vast majority of the South African coalbed seams are located in the Main Karoo basin, particularly in the northeastern regions, including Mpumalanga, KwaZulu–Natal, and Free State provinces [40]. Two coal samples were used in this study: (1) Ermelo coal (denoted RL and sourced from Mpumalanga province) and (2) Somkhele (denoted SK and sourced from KwaZulu-Natal province), as shown in Figure 1. To determine the coal identification, the samples were characterised using proximate and ultimate analysis, as well as petrographic composition. A thermogravimetric analyser (TGA701 Leco) was used to conduct a proximate analysis following the International Organization for Standardization (ISO) procedures 11,722:2013 for moisture, 1171:2010 for ash, 562:2010 for volatile matter, and the fixed carbon was found by difference. The ultimate analysis was performed using the Leco CHN and Leco S instruments following the ISO 17,247:2013 procedure, while the O content was determined by differences in the C, H, N, and S.

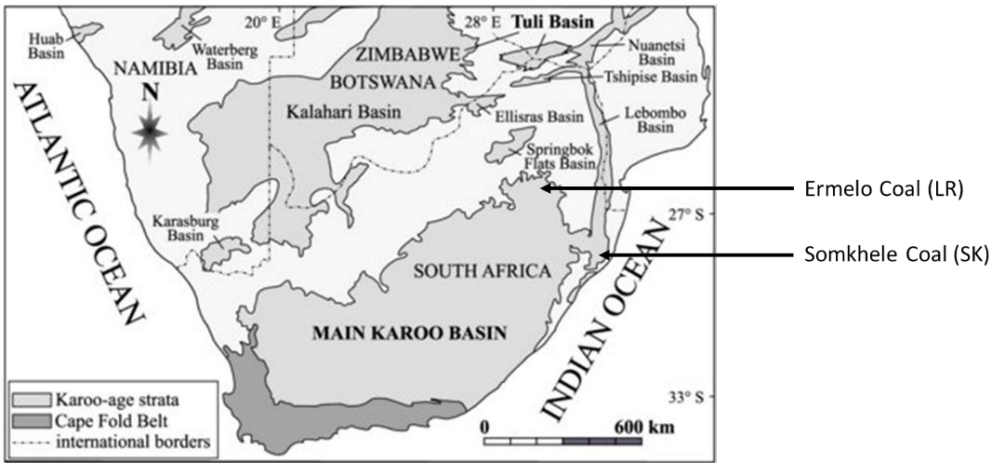


Figure 1. The South African Main Karoo Basin (adopted with permission from Bordy and Catuneanu [41]).

The coals were collected from the coalfields as fresh core samples; they were flushed with nitrogen and conserved in sealed plastic containers to prevent adverse oxidation and exposure to atmospheric moisture. The analytical data of the two coal samples are presented in Table 1. The results, i.e., the proximate analysis, show that Coal SK from the KwaZulu–Natal region has high fixed carbon (74.1 wt.%) and low volatile matter (7.6 wt.%), which can be categorised as anthracite coal (Anthracite C), with respect to the mean vitrinite reflectance of 2.23%. In contrast, Coal RL from the Mpumalanga region has low fixed carbon (27.8 wt.%) and high volatile matter (49.8 wt.%), which is classified as bituminous coal (Bituminous C). Carbon dioxide gas was used as the adsorbate with a purity of 99.999% and was acquired from Afrox Oxygen Ltd. The details of the chemical structural properties of the two coals using advanced analytical techniques are given in our previous work [42], where we probed their textural properties, surface chemistry, morphology, and crystallinity.

Table 1. Petrographic, proximate, and ultimate composition of the two coal samples.

	Maceral Composition (vol.%, mmf)				Proximate Analysis (wt.%, adb)				Ultimate Analysis (wt.%, adb)				
Coal ID	**Vitr.**	**Lipt.**	**Inert.**	**R_oV%**	**M**	**A**	**VM**	**FC**	**C**	**H**	**N**	**S ***	**O**
RL	12.8	3.3	74.2	0.64	4.5	17.9	49.8	27.8	75.1	4.6	1.9	0.6	17.8
SK	84.0	0.0	11.5	2.24	1.0	17.3	7.6	74.1	82.0	3.1	1.9	0.9	12.1

Vitr.—vitrinite; Lipt.—liptinite; Intert.—inertinite; R_oV—mean vitrinite reflectance; adb—air-dried basis; mmf—mineral matter free; M—moisture; A—ash; FC—fixed carbon; VM—volatile matter; C—carbon; N—nitrogen; H—hydrogen; and S *—total sulphur.

The pore structure properties of the two coals were measured using the Micromeritics ASAP 2020 surface area and porosity analyser and are presented in Table 2. This was conducted through the carbon dioxide low-pressure gas adsorption technique (CO_2-LPGA) using the Brunauer–Emmett–Teller (BET) and Langmuir methods for the specific surface area, the Dubinin–Radushkhevic (D-R) for the micropore surface area, and the Horvath–Kawazoe (H-K) for both micropore volume and average micropore diameter. Coal SK has the largest specific surface area of 114.3 m^2/g compared to Coal RL, with 77.4 m^2/g. It is often anticipated that vitrinite-rich coal has more surface area than inertinite-rich coal [43]. Subsequently, the micropore surface area and volume, as well as the average micropore diameter, are greater for Coal SK than Coal RL. The average micropore diameters of both coals suggest that there are dense microporous regions within the pore structures, as per the International Union of Pure and Applied Chemistry (IUPAC) notation [44].

Table 2. Textural properties of the two coal samples.

	Specific Surface Area (m^2/g)		Micropore Specific Surface Area (m^2/g)	Micropore Volume $\times 10^{-2}$ (cm^3/g)	Average Micropore Diameter (Å)
Coal ID	**BET**	**Langmuir**	**D-R**	**H-K**	**H-K**
RL	77.4 ± 2.2	82.3 ± 3.3	116.7	0.0273	3.74 ± 0.06
SK	114.3 ± 1.2	121.8 ± 2.2	181.9	0.039723	4.21 ± 0.04

2.2. Measurement of Adsorption Isotherms

The supercritical sorption experiments were measured using a high-pressure volumetric adsorption system (HPVAS) designed, constructed, and commissioned by Premlall et al. [45] and followed the experimental procedure originally developed and published by Mabuza et al. [17]. The approach required a sample preparation step in which the samples are crushed to a sieve size between 2 mm and 1 mm and degassed under a vacuum for 24 h at 105 °C, as recommended by Zhao et al. [46]. To ensure the reliability and repeatability of the adsorption isotherm measured, each experiment was carried out three times using the same incremental pressure steps to a maximum (9.0 MPa). Subsequently, the standard deviation of the isotherm measurements was calculated and averaged at ±0.02 at each temperature tested, thus suggesting results with good repeatability.

2.3. Non-Linear Three-Parameter Isotherm Models

It is very common in the published literature that the analytical isotherms used for modelling the adsorption of single-gas CO_2 for porous adsorbents, including coal, are the linearised two-parameter Langmuir, Freundlich, Temkin, and Dubinin–Radushkevich [47–49]. Due to their ease of linearisation, two-parameter models are typically chosen despite their simplicity. On the other hand, fitting becomes distorted and parameter estimation errors occur when non-linear isotherm equations are transformed into linear forms [50]. This study employed non-linear regression three-parameter models, including Sips, Tóth, and Dubinin–Astakhov (DA). These models are rigorous and are able to model gas–solid sorption systems for

both homogeneous and heterogeneous distributions, both at low and high pressures [51]. Furthermore, the nonlinear optimisation approach does not transform the dataset. Hence, the original error distribution remains undistorted. Therefore, the three nonlinear isotherms were analysed using the OriginPro software tool.

2.3.1. Langmuir–Freundlich (Sips) Model

In addition to adopting some of the fundamental assumptions of the Langmuir model, the Langmuir–Freundlich (LF) (Sips) isotherm takes surface heterogeneity into account, which makes it capable of modelling both homogeneous and heterogeneous binding sites [52]. The Sips integrates the knowledge of adsorption on heterogeneous surfaces. It reveals how adsorption energy is distributed throughout the heterogeneous surface of the adsorbent [30]. Another advantage of the LF model is that the number of binding sites does not need to be measured independently, which may be difficult for a complex and heterogeneous material like coal. This makes it one of the most useful and practical models for adsorption equilibria studies [52]. The model is more relevant to the current study since it was originally proposed for systems involving gas adsorption on heterogeneous solids. The non-linear Langmuir–Freundlich isotherm model may be expressed as follows:

$$n_s = \frac{N_{sm}(K_{LF}P)^n}{1 + (K_{LF}P)^n} \tag{1}$$

where n_s (mmol/g) is the adsorbed amount at equilibrium, N_{sm} (mmol/g) is the potential maximum adsorption capacity, which is directly linked to the number of binding sites available, n (-) is the heterogeneity parameter, P (MPa) is the system pressure at equilibrium, and K_{LF} (MPa^{-1}) is the Langmuir–Freundlich constant, which is also referred to as the affinity constant for adsorption. According to Babatunde et al. [53] the index of heterogeneity, n, should lie between 0 and 1 for a heterogeneous solid surface.

2.3.2. Tóth Model

The Tóth isotherm was introduced in the early 1960s to better describe adsorption on heterogeneous surfaces. The Tóth isotherm model is another useful variation of the Langmuir model that improves the predicted value's agreement with experimental results by accounting for the presence of multilayer and sub-monolayer coverage. Similar to the Langmuir–Freundlich models, the Tóth model was initially proposed to describe the gas–solid adsorption equilibrium systems before it was used for solid–solution systems [54]. It is employed to characterise adsorption on heterogeneous surfaces at both low and high adsorbate concentrations/pressures. The major assumption of the Tóth model is an asymmetrical quasi-Gaussian energy distribution that is extended towards low sorption energies [55]. The non-linear Tóth model equation is generally applied in the following form [56]:

$$n_s = \frac{N_{sm}K_TP}{\left(1 + (K_TP)^{n_T}\right)^{\frac{1}{n_T}}} \tag{2}$$

where N_{sm} (mmol/g) is the maximum adsorption capacity, n_s (mmol/g) is the adsorbed amount at equilibrium, K_T (MPa^{-1}) is the Tóth isotherm model constant (MPa^{-1}), P (MPa) is the equilibrium pressure, and n_T (-) is the dimensionless equilibrium constant that described the heterogeneity of the adsorbent. The characteristic of the heterogeneity of the adsorption system is represented by the parameter n_T, such that, when n_T is unity, it suggests that the surface is homogeneous and the comparative energies of the different adsorption sites are the same. Hence, the Tóth equation is similar to the Langmuir equation.

2.3.3. Dubinin–Astakhov Model

The Dubinin–Astakhov (DA) model was developed as a semi-empirical model motivated by the Weibull distribution of the adsorption potential. The D-A model is an extension of the Dubinin–Radushkhevich (D-R), and it considers the surface heterogeneity of microporous adsorbents with a larger size distribution [57]. The equations for the two models are similar except that the D-A equation has the superscript n instead of 2 for D-R [53]. Thus, the D-A equation is given by the following expression:

$$W = W_0 \exp\left\{-\left[\frac{RT}{E} ln\left(\frac{P_0}{P}\right)\right]^n\right\} \quad (3)$$

where W (mmol/g) is the amount adsorbed at equilibrium, T (K) is the isothermal temperature, W_0 (mmol/g) is the maximum adsorption capacity at equilibrium temperature and pressure, P_0 (MPa) is the saturation pressure, P (MPa) is the equilibrium pressure, E (kJ/mol) is the activation energy, R (kJ/mol·K) is the universal gas constant, and n (-) is the Dubinin–Astakhov coefficient. The distribution parameter, n, is often called a surface energy heterogeneity factor, which is related to the heterogeneity of the adsorbent [58].

2.4. Error Analysis

Variation between the experimental data and the estimated (model) values may be described by error analysis methods [59]. To avoid and minimise foreseeable statistical biases, Ayawei et al. [30] recommends that multiple error analysis methods be used for the same set of data. Therefore, three error analytical methods were used to evaluate the data to determine the best-fitting isotherm model, including root-mean-square deviation (RMSD), the non-linear chi-square (χ^2) test, and the error of regression (EoR). Another commonly used factor that was used in this analysis is the coefficient of determination (R^2). Although R^2 is a very simple tool, it has been used in reporting a number of statistical analyses. However, Renaud and Victoria-Feser [60] suggest that R^2 should not be applied as a final model validation or selection tool, but it should be considered as a guideline that indicates if the selected explanatory factors are appropriate for predicting the response. According to Asuero et al. [61] a coefficient of determination with a strength ranging from 0.90 to 1.00 suggests that the experimental and theoretical data are highly correlated.

The root-mean-square deviation (RMSD) between the model values and the experimental data is mathematically expressed as:

$$RMSD = \sqrt{\frac{\sum_{i=1}^{N} \left(Q_{exp} - Q_{mod}\right)^2}{N}} \quad (4)$$

While the chi-square (χ^2) test was evaluated using the following mathematical definition,

$$\chi^2 = \sum_{i=1}^{N} \frac{\left(Q_{mod} - Q_{exp}\right)^2}{Q_{exp}} \quad (5)$$

and, finally, the following equation was used to determine the percentage error of regression ($EoR\%$) [62]:

$$EoR\% = \frac{\sqrt{\frac{1}{N}\sum_{i=1}^{N} \left(Q_{exp} - Q_{mod}\right)^2}}{\frac{1}{N}\sum_{i=1}^{N} Q_{exp}} \times 100\% \quad (6)$$

In Equations (4)–(6), Q is the number of moles, N is the number of data points, and the subscripts 'exp' and 'mod' are the experimental and model values, respectively.

2.5. Clausius–Clapeyron Approach for Isosteric Heat of Adsorption

One important factor in the design of adsorptive gas separation processes is the isosteric heat of adsorption of a gas. It offers the necessary binding strength needed for the adsorption process [63]. The isotherms at two or more different temperatures may be measured experimentally in order to determine the differential enthalpy of adsorption at constant coverage, often referred to as the isosteric approach [64]. The isosteric enthalpy of adsorption, $Q_{st,i}$, (kJ/mol), may be evaluated using the Clausius–Clapeyron equation [65]:

$$Q_{st,i} = RT^2 \left(\frac{\partial \ln P}{\partial T} \right)_{n_i} \tag{7}$$

where P (kPa) is the equilibrium gas phase pressure, R is the universal gas constant, T (K) is the isothermal temperature, and n_i (mmol/g) is the amount of gas adsorbed at equilibrium. The Clausius–Clapeyron equation considers two key assumptions [66]. (1) The volume of the adsorbed phase is negligible since it is very small compared to the gas phase volume, and (2) the bulk gas phase behaves as an ideal gas. Another useful form of the Clausius–Clapeyron equation is given by [67]:

$$\frac{Q_{st,i}}{R} = \left(\frac{\partial \ln P}{\partial (1/T)} \right)_{n_i} \tag{8}$$

Integrating gives the linear form of the equation,

$$\ln P = -\frac{Q_{st,i}}{RT} + C \tag{9}$$

such that C is the integration constant, and $Q_{st,i}$ is then evaluated from the straight-line slopes from plotting the natural log pressure ($\ln P$) versus the reciprocal of the isothermal temperature ($1/T$) at a specific fixed amount of gas adsorbed [68].

3. Results and Discussion

3.1. Characteristics of the Gas Sorption Equilibrium Isotherms

The high-pressure supercritical CO_2 experimental isotherm results for Coal RL and Coal SK are presented in Figure 2a–d at various temperatures. Both of the samples yielded Type I adsorption isotherms with an increase in sorption capacity at 6.0 MPa and then reached an asymptotic trend from 6.0 to 9.0 MPa. This suggests that equilibrium saturation was achieved at subcritical pressures, i.e., pressures < 7.38 MPa throughout the temperature range considered. As demonstrated in Figure 3, the phenomenon through which sorption isotherms exhibit a monotonous asymptotic behaviour occurs when the bulk density of the gas phase starts to increase rapidly as a function of pressure towards approaching the adsorbed phase density. Dutta et al. [69] observed similar behaviour when investigating the sorption characteristics of Indian coals from the Jharkhand and West Bengal states.

Figure 2 also shows that the maximum excess sorption capacity for low-ranked Coal RL ranges from 2.25 to 3.46 mmol/g, which was found to be lower than that of high-ranked Coal SK, which ranges from 2.54 to 4.16 mmol/g. High-ranked vitrinite-rich coals tend to exhibit a large specific surface area in the microporous region, which is associated with excellent CO_2 interaction, and this results in a high CO_2 sorption capacity compared to low-ranked inertinite-rich coals [70]. A negative temperature effect is also observed, with the sorption capacity decreasing with an increase in temperature. The negative temperature

influence is due to the exothermic nature of the adsorption process, which is favourable at lower temperatures [71]. The overall reduction in CO_2 sorption due to increased temperature is more pronounced for high-ranked Coal SK at 39.0% than for low-ranked Coal RL at 35.0%. High-ranked coals are more susceptible to this negative temperature effect since they have enhanced affinity for CO_2 than low-ranked coals, resulting in a drastic drop in the CO_2 sorption capacity under increased temperature conditions, driven by the kinetic energy of the gas molecules and the consequent desorption [13,72].

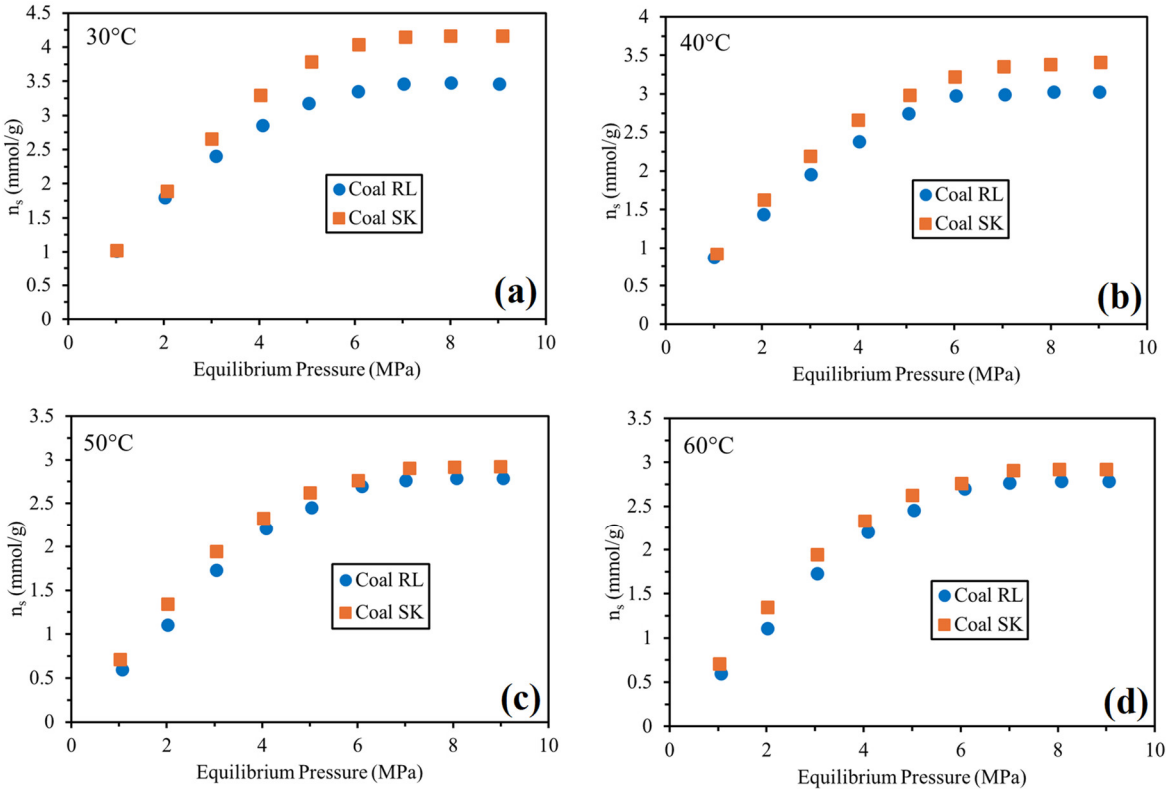


Figure 2. Experimental isotherms for Coals RL and SK at (**a**) 30 °C; (**b**) 40 °C; (**c**) 50 °C; and (**d**) 60 °C.

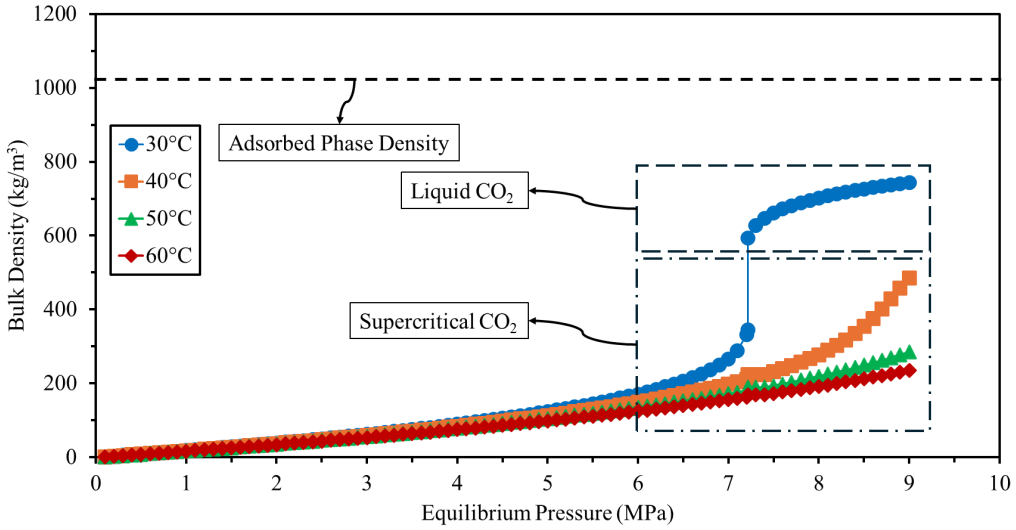


Figure 3. Bulk phase CO_2 density profile from 30 °C to 60 °C.

3.2. Modelling of the Adsorption Isotherms

The predicted isotherms for CO_2 sorption on Coal RL and Coal SK from 30 °C to 60 °C, established using the non-linear three-parameter regression models including Dubinin–

Astakhov (DA), Langmuir–Freundlich, and Tóth, are shown in Figure 4, Figure 5, and Figure 6, respectively. The data points represent the experimental data, while the solid lines are the model regressions. The estimated isotherm parameters for the respective models and their corresponding coefficients of determination (R^2), and the statistical evaluations, including root-mean-square deviation (RMSD), the non-linear chi-square (χ^2) test, and the error of regression (EoR), are presented in Table 3 at the various temperatures considered. This residual analysis was conducted to quantitatively compare and determine the isotherm model that best fits the experimental data.

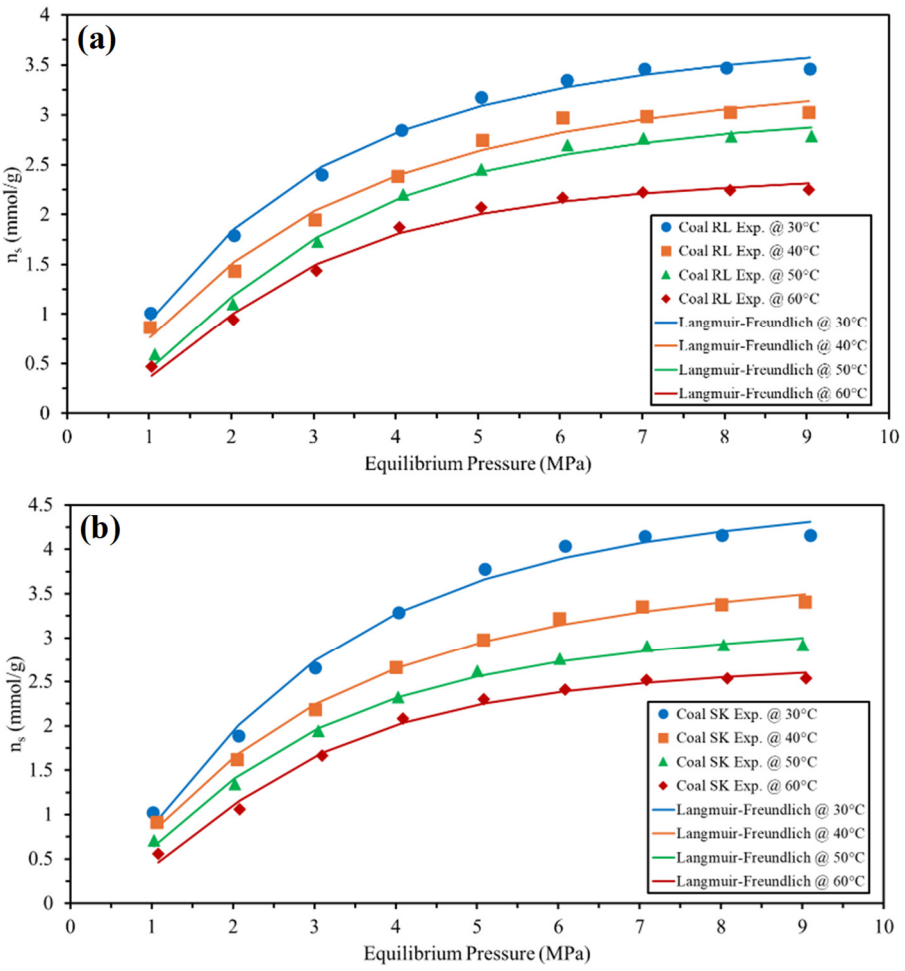


Figure 4. Predicted isotherms for CO_2 sorption on coal from 30 °C to 60 °C using the Langmuir–Freundlich three-parameter non-linear regression model: (**a**) Coal RL and (**b**) Coal SK.

Table 3. Dubinin–Astakhov, Langmuir–Freundlich, and Tóth isotherm models parameters for CO_2 sorption on Coals RL and SK.

		Coal RL				Coal SK			
Model	**Isotherm Parameter**	**30 °C**	**40 °C**	**50 °C**	**60 °C**	**30 °C**	**40 °C**	**50 °C**	**60 °C**
Langmuir–Freundlich(Sips)	N_{sm} (mmol/g)	4.030	3.661	3.177	2.485	4.859	4.046	3.336	2.814
	K_{LF} (MPa^{-1})	0.443	0.389	0.373	0.408	0.390	0.386	0.410	0.400
	n	0.674	0.700	0.540	0.503	0.614	0.677	0.600	0.513
	R^2	0.993	0.986	0.993	0.991	0.990	0.995	0.995	0.993
	RMSD (±)	0.070	0.090	0.066	0.059	0.107	0.058	0.051	0.057
	χ^2	0.018	0.040	0.036	0.037	0.048	0.014	0.016	0.033
	EoR (%)	2.512	3.805	3.107	3.398	3.295	2.197	2.262	2.923

Table 3. *Cont.*

Model	Isotherm Parameter	Coal RL				Coal SK			
		30 °C	40 °C	50 °C	60 °C	30 °C	40 °C	50 °C	60 °C
Tóth	N_{sm} (mmol/g)	3.806	3.179	2.822	2.246	4.266	3.619	3.008	2.549
	K_T (MPa^{-1})	0.062	0.011	0.000	0.000	0.002	0.018	0.005	0.000
	n_T	2.105	3.091	5.483	6.720	4.181	2.716	3.584	5.540
	R^2	0.999	0.999	0.999	0.999	0.999	0.999	0.999	0.999
	RMSD (±)	0.054	0.065	0.024	0.017	0.042	0.033	0.019	0.028
	χ^2	0.009	0.031	0.003	0.002	0.010	0.005	0.001	0.005
	EoR (%)	1.956	2.745	1.109	0.981	1.307	1.262	0.863	1.463
Dubinin–Astakhov	W_0 (mmol/g)	3.447	3.091	2.953	2.479	4.115	3.448	3.081	2.781
	E (kJ/mol)	5.426	5.243	4.690	5.087	4.799	5.107	5.204	5.058
	n	1.000	1.000	1.000	1.000	1.000	1.000	1.000	1.000
	R^2	0.994	0.994	0.991	0.989	0.992	0.995	0.993	0.990
	RMSD (±)	0.224	0.196	0.219	0.197	0.298	0.203	0.205	0.210
	χ^2	0.199	0.164	0.260	0.262	0.303	0.176	0.219	0.266
	EoR (%)	8.065	8.245	10.305	11.335	9.208	7.692	9.042	10.680

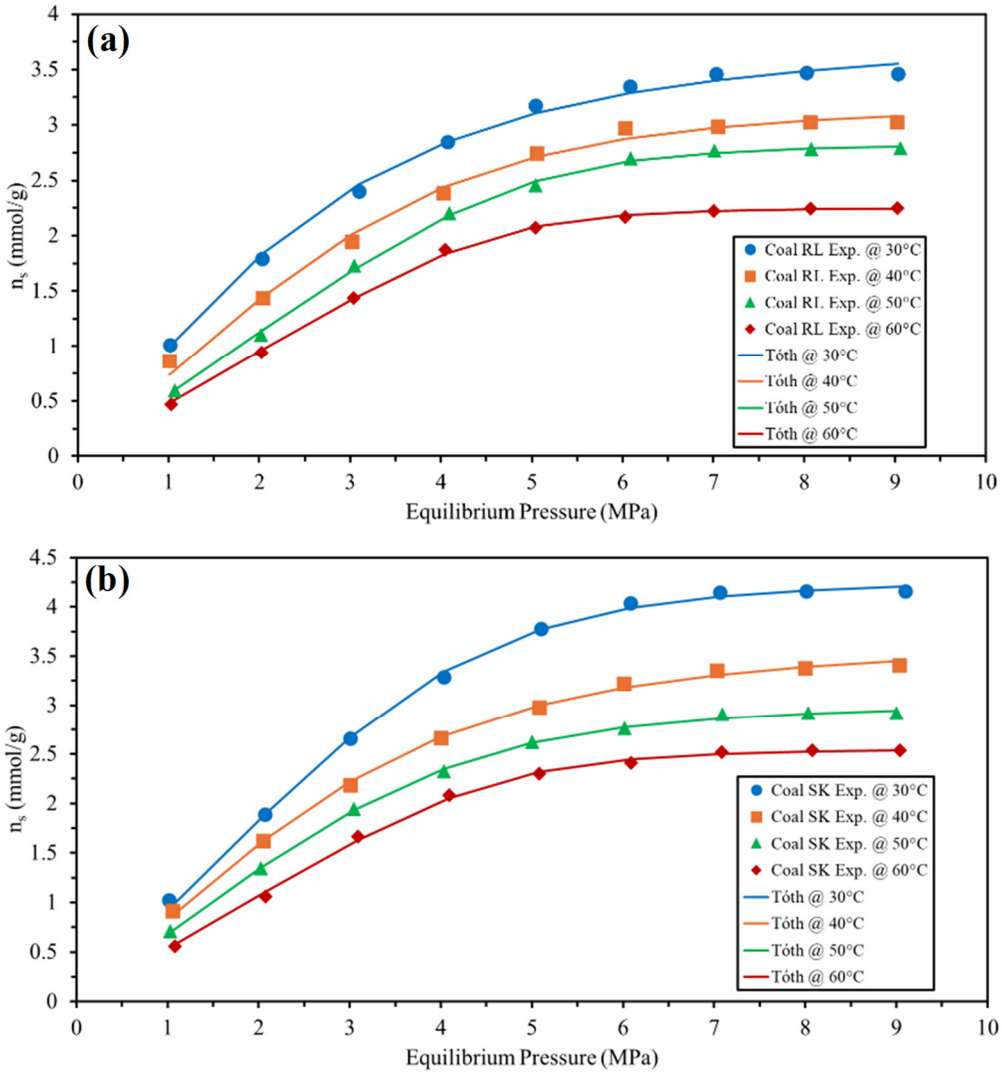


Figure 5. Predicted isotherms for CO_2 sorption on coal from 30 °C to 60 °C using the Tóth three-parameter non-linear regression model: (**a**) Coal RL and (**b**) Coal SK.

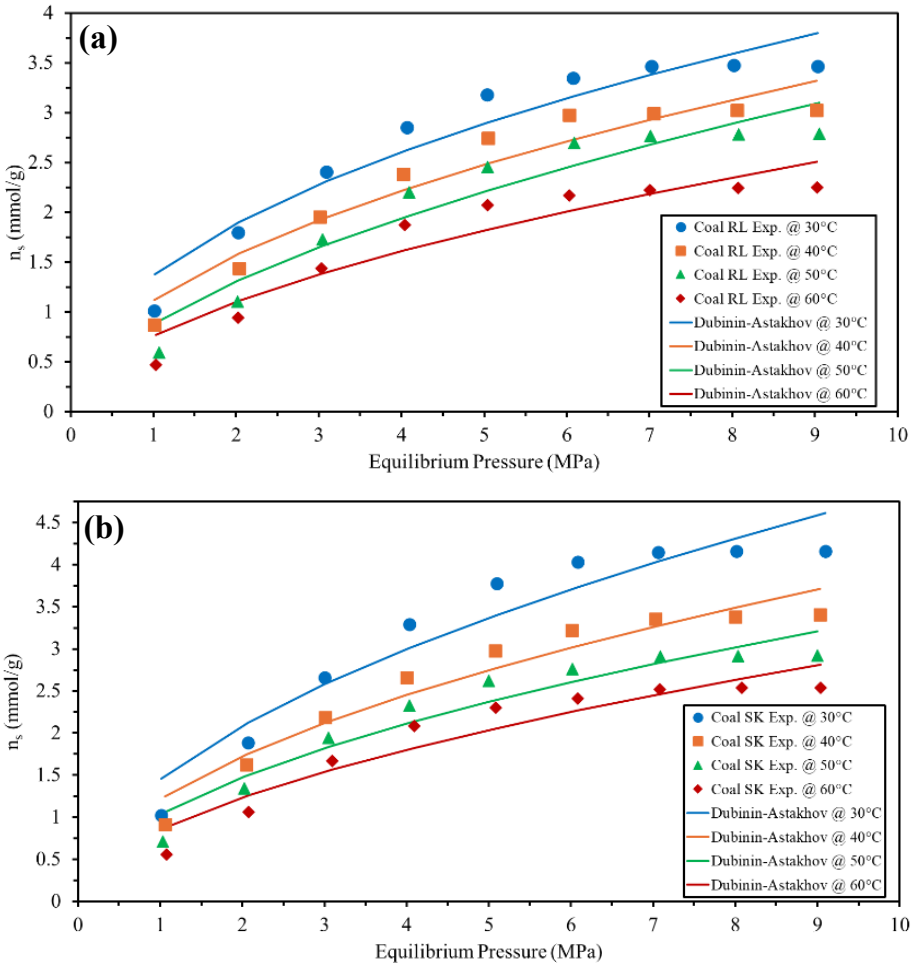


Figure 6. Predicted isotherms for CO_2 sorption on coal from 30 °C to 60 °C using the Dubinin–Astakhov three-parameter non-linear regression model: (**a**) Coal RL and (**b**) Coal SK.

The Langmuir–Freundlich (Sips) and Tóth models, in Figures 4 and 5, respectively, show a good and consistent fit of the experimental data at all temperatures and throughout the entire pressure range. There are some deviations between the model and the experimental data for Sips, particularly at supercritical pressures. This occurrence is common when applying the Sips model at high pressures [51]. Although the Sips model may present some deviations, particularly at higher pressure, it offers insights into the heterogeneity of the adsorption sites and the distribution of energy accessible for adsorption on the adsorbent surface. These deviations are insignificant. Thus, the Sips model may also be considered to describe the experimental data with acceptable accuracy.

The Tóth model exhibits a higher level of correlation with the experimental data throughout the whole spectrum of adsorption temperatures and pressures. Although both the Sips and Tóth models have coefficients of determination above 0.900, the Tóth model's R^2 values may be approximated to unity since they are all at 0.999. The Tóth RMSD values range from 0.017 to 0.065, which are very large compared to the Sips values, which range from 0.051 to 0.107, considering both the coals. Furthermore, the nonlinear χ^2 values are in the range of 0.014–0.048 for Sips and 0.001–0.031 for Tóth, while the EoR values for the respective models are 2.197–3.805% and 0.863–1.956%. The differences in the residual analysis for the two models suggest that the nonlinear Tóth model more effectively characterises the experimental CO_2 adsorption isotherms on Coal RL and Coal SK. The Tóth model's data fit outcomes were expected since Abdulsalam et al. [73] allude that the Tóth model is effective in characterising heterogeneous adsorption systems, as it covers both low and high-end pressure requirements and accurately characterises many systems

with sub-monolayer coverage. These findings allow for a general classification of the three models for CO_2 as follows: *Tóth* > *Langmuir–Freundlich (Sips)* > *Dubinin–Astakhov (DA)*. This classification corresponds to and adds to that of Serafin et al. [74], in which their classification order was as follows for CO_2: *Tóth* > *Sips* > *Langmuir* > *Freundlich* > *Temkin* at temperatures ranging from 0 to 40 °C.

The model parameters for Sips and Tóth, as presented in Table 3, allow for the comprehensive understanding of the mechanism and nature of the CO_2 sorption process on the coal surfaces. The potential maximum adsorption capacity (N_{sm}), which is directly linked to the number of binding sites available, decreases with the increased adsorption system temperature for both the Sips and Tóth models due to weakened attractive forces between the coals and CO_2, specifically the London dispersion forces associated with the CO_2–coal attractions [75]. For Sips, the values decreased from 4.030 to 2.485 mmol/g for Coal RL and from 4.859 to 2.814 mmol/g for Coal SK. Similarly, for Tóth, the model estimated a decrease from 3.806 to 2.246 mmol/g for Coal RL and from 4.266 to 2.549 mmol/g for Coal SK. This consistent phenomenon confirms that the CO_2–coal sorption system is a highly exothermic process, as demonstrated by the negative temperature influence earlier. Additionally, the theoretical potential maximum CO_2 adsorption capacity values are in proximity to the experimental equilibrium adsorbed amount, N_s, values reported earlier, which ranged between 2.250 and 3.460 mmol/g for Coal RL and between 2.540 and 4.160 mmol/g for Coal SK. When the N_s and N_{sm} values correlate well within proximity, it suggests that the isotherm models applied prove some high level of reliability [76].

The Sips heterogeneity parameter (n) indexes fall within 0 and 1 for Coal RL and Coal SK, averaging at 0.604 and 0.601, respectively. This confirms that both coals have heterogeneous solid surfaces and that CO_2 sorption on the coals occurred by physical adsorption. This is corroborated by the Tóth model equilibrium constant (n_T) values that deviate far from the state of unity (i.e., all above 2.000), which then implies that the adsorption system takes place heterogeneously on the solid surface, with the adsorption sites having relatively distinct energies. Thus, the Tóth model cannot be reduced to the Langmuir isotherm. The values of the affinity parameter for adsorption (K_{LF}) for the Sips model vary between 0.373 and 0.443 MPa^{-1} for Coal RL, and 0.390 and 0.410 MPa^{-1} for Coal SK, implying favourable CO_2 adsorption and that the Sips equation cannot be reduced to the Freundlich. According to Belhachemi and Addoun [77], the values of K_{LF} approaching zero reduce the Langmuir–Freundlich equation to simply the Freundlich. The calculated affinity parameter values acquired through the Tóth model indicate a decreasing trend with an increase in temperature, while approaching zero at higher temperatures. This explains that CO_2 adsorption on the coals was strongly favourable at lower temperatures. Abdulsalam et al. [62] observed a similar trend when studying CO_2 adsorption mechanisms onto Malaysian coals under different temperature conditions through the application of the Tóth model. Increased adsorption system temperature weakens the London dispersion forces associated with CO_2–coal attractive forces, consequently compromising the affinity of the coals for CO_2.

Overall, the DA showed a poor to fair fit for the sorption data for both of the coals tested, as shown in Figure 6. The DA model significantly overpredicted the sorption data at low and supercritical pressures, while underprediction was observed at subcritical pressures. This is quite unexpected, considering that the coefficient of determination (R^2) values of the DA plots for both coals were notably high (0.989–0.995), as shown in Table 3. This inconsistency indicates that a strong correlation in the DA plot does not necessarily guarantee the model's accuracy in representing the sorption data. One of the key assumptions of the DA model is related to the adsorbate molecules filling the micropores of the adsorbent, occupying the available active sites and volume [78]. Thus,

this poor DA data fit suggests that the adsorption mechanism in the micropore regions is primarily driven by layer-by-layer surface coverage rather than pore filling.

Alexander et al. [79] strongly warns against excessively relying on the R^2 to measure goodness-of-fit in model regressions and suggests that the R^2 value seemingly appears to be primarily mathematical, lacking substantial practical relevance, particularly in nonlinear regressions. This is further justified by the high error of regression (EoR) values, which range between 7.692 and 11.335% for the two coals. The weakness of the DA is further shown to be prevalent by the characteristic value of the activation energy (E), which is distinctly changing with the temperature, as shown in Table 3, and it should be practically independent of the temperature [80,81]. However, this phenomenon may not be elucidated by the mathematical inaccuracies of the DA model but by the lack of a complementary fit between the model and the experimental data. Consequently, these findings imply that the DA nonlinear model cannot be used to predict the sorption behaviour of the two coals under the experimental conditions investigated. Hence, the calculated activation energy (E) values would merely be used as guidelines in adsorption system design and optimisation rather than for accuracy purposes. These findings allow for a general classification of the three models for CO_2 as follows: *Tóth > Langmuir–Freundlich (Sips) > Dubinin–Astakhov (DA)*. This classification corresponds to and adds to that of Serafin et al. [74], in which their classification order was as follows for CO_2: *Tóth > Sips > Langmuir > Freundlich > Temkin* at temperatures ranging from 0 to 40 °C.

3.3. Adsorption Thermodynamics of CO_2 onto the Coals

As mentioned in the earlier sections, the amount of heat released during exothermic processes, the isosteric heat of adsorption, is used to measure such physisorption. The isosteric heat of adsorption complements the CO_2 adsorption equilibrium studies and was calculated using the Clausius–Clapeyron equation for the tested coal samples. To conduct this, the adsorption isosteres were generated from the sorption equilibrium data, as shown in Figure 7, with nine different fractional uptake loadings ranging from 0.4 to 3.6 mmol/g to cover the minimum and maximum sorption capacity range of the isotherms acquired experimentally. It is also noted in Figure 7 that the adsorption isosteres have negative gradients with positive y-intercepts, as is often the case for gas–solid sorption systems on heterogeneous surfaces [67,82]. The slope from the isostere is used to determine the differential isosteric enthalpy of adsorption (Q_{st}), as illustrated in Figure 8. Skoczylas et al. [83] infer that the magnitude of the interaction between the solid and the adsorbate determines the heat of adsorption, and the extent of hydroxyl groups on coal surfaces is correlated with its value.

Figure 8 shows a linearly increasing trend of the isosteric heat as the adsorption process proceeds at different CO_2 uptake loadings for both coals, namely SK and RL. Huang et al. [82] recently observed similar findings on the class of coals from the Qinshui coalfield in Shanxi Province, Changzhi City, China, in which they attributed this behaviour to a more-pronounced CO_2–coal interaction, particularly at supercritical pressures, which is common for gas–solid sorption systems. The heat released responds to different CO_2–coal interactions due to the chemical nature and porosity of the coal [64]. The isosteric heat values and their increasing trajectory are different for each coal studied. Coal SK has the highest heat of adsorption (37.408 kJ/mol at CO_2 uptake of 3.60 mmol/g) and also has the lowest (7.518 kJ/mol at CO_2 uptake 0.40 mmol/g). For Coal RL, the respective heats of the adsorption values were found to be 34.600 kJ/mol and 14.500 kJ/mol. The different structural and petrographic characteristics of the coals under study account for the variations in these values. The specificity of coal–sorbate particle interactions is impacted by these variations, although both show a linear behaviour. Coal RL is low-ranked with a high content of inertinite group in its maceral clusters, suggesting a low degree of coalification

and indicating firmness in the coal matrix and, thus, having energetically low sorption sites for CO_2 adhesion on the coal surface. For the high-rank and vitrinite-rich Coal SK, the CO_2 molecules tended to adsorb on the high-energy sites even at subcritical pressures, consequently releasing more heat as the adsorption process proceeds, which corresponds to the physical interactions between CO_2 molecules and the coal [84].

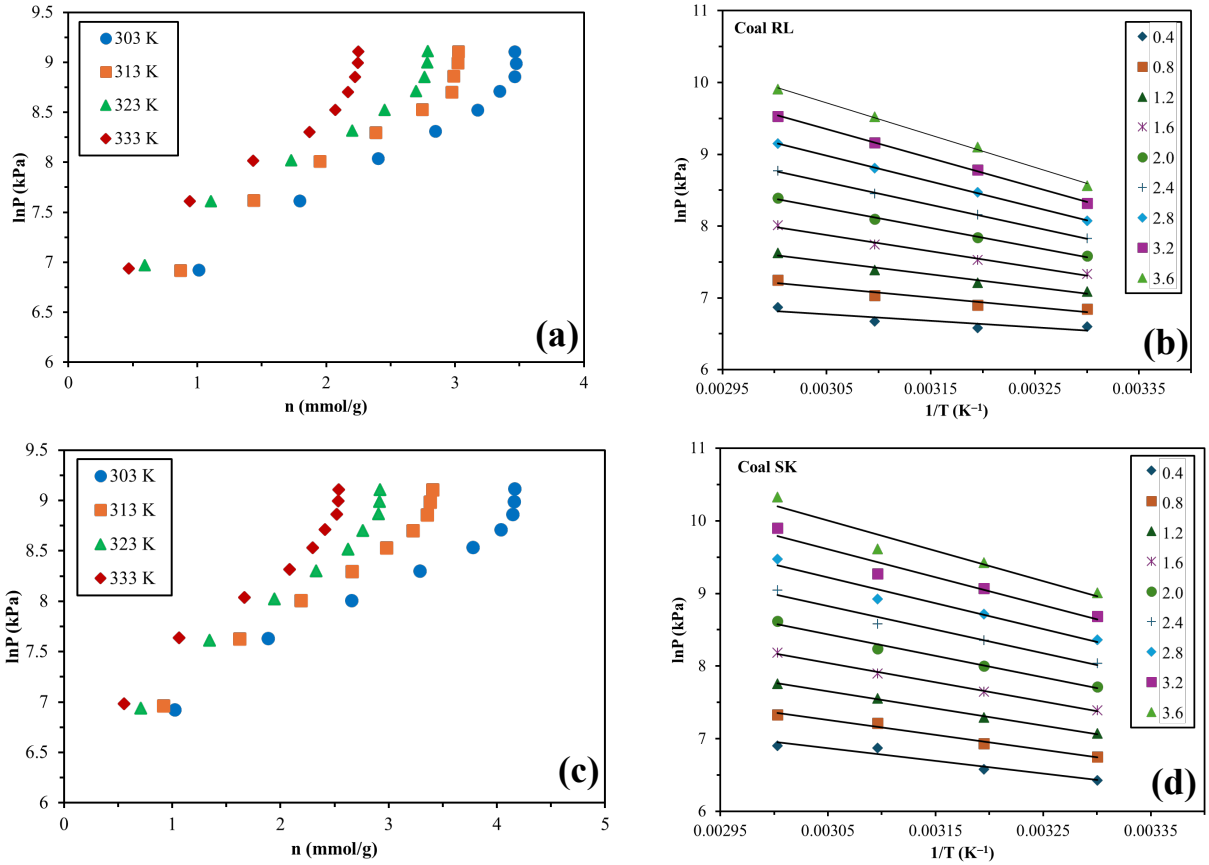


Figure 7. Adsorption isosteres (lnP against 1/T) represented from the temperatures of 30 °C to 60 °C for 9 different uptake loadings: (**a**,**b**) Coal RL; and (**c**,**d**) Coal SK.

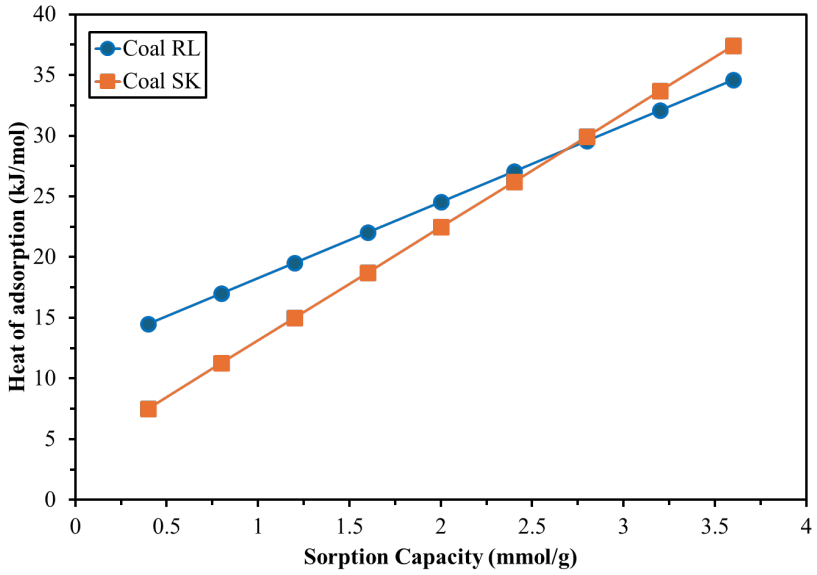


Figure 8. Change of isosteric heat of adsorption with sorption capacity in the adsorption process for Coal RL and Coal SK.

4. Conclusions

The study presented carbon dioxide (CO_2) supercritical sorption measurements carried out at temperatures ranging from 30 °C to 60 °C and pressures up to 9.0 MPa on bituminous and anthracite coals from South African coalfields. The Sips, Tóth, and Dubinin–Astakhov (DA) three-parameter isotherm models were applied in their nonlinear form as well as the Clausius–Clapeyron equation for thermodynamics evaluation. The following conclusions were drawn:

- The maximum sorption capacities show a negative temperature effect and exhibit a positive trend with the increase in coal rank and vitrinite content. Thus, Coal SK has a higher sorption capacity than Coal RL. This means that Coal SK has a great potential as a suitable candidate coal for long-term CO_2 sequestration in unmineable seams based on the compatible sorption characteristics;
- Both coals have shown that the excess sorption isotherm data generated under in situ reservoir conditions can be well-modelled by the Langmuir–Freundlich (Sips) and Tóth adsorption isotherm models. However, the Dubinin–Astakhov (DA) model is unable to describe the same data under comparable conditions. Generally, the appropriateness of fit in the three models applied decreased in the following order: *Tóth* > *Sips* > *DA* based on their combined residual analysis. This consistency between the experimental and model results indicates that the Sips and Tóth models are the most practicable for predicting the sorption behaviour by nonlinear regression, further suggesting that these models may be practically applicable when simulating CO_2–coal sorption systems using various simulation-based tools;
- From the sorption thermodynamics of the study, the isosteric heat of adsorption for CO_2 on the coals exhibits an upward trend with increasing adsorption loading, suggesting that the primary interactions among the adsorbed CO_2 molecules are interactive forces. This implies that the coal matrix has many molecular levels of CO_2 adsorption with different energy intensities.

Author Contributions: Conceptualisation, M.M.M. and M.G.R.M.; methodology, M.M.M.; validation, M.M.M. and M.G.R.M.; formal analysis, M.M.M. and M.G.R.M.; investigation, M.M.M.; resources, M.M.M.; data curation, M.M.M.; writing—original draft preparation, M.M.M.; writing—review and editing, M.M.M. and M.G.R.M.; visualisation, M.M.M. and M.G.R.M.; project administration, M.M.M.; funding acquisition, M.M.M. All authors have read and agreed to the published version of the manuscript.

Funding: This research was funded by the National Research Foundation (NRF) of South Africa, grant number TTK2204224344. The APC was funded by the University of Johannesburg.

Data Availability Statement: The authors will provide the raw data used to support the results in this article upon request.

Acknowledgments: The authors acknowledge the Tshwane University of Technology and Kasturie Premlall for the research facilities (high-pressure volumetric adsorption system).

Conflicts of Interest: The authors declare no conflicts of interest. The funders had no role in the design of the study; in the collection, analyses, or interpretation of data; in the writing of the manuscript; or in the decision to publish the results.

Abbreviations

The following abfbreviations are used in this manuscript:

SK	Somkhele Coal
RL	Ermelo Coal
HPVAS	High-pressure volumetric adsorption system

L-F	Langmuir–Freundlich
DA	Dubinin–Astakhove
D-R	Dubinin–Radushkhevich
RMSD	Root-mean-square deviation
EoR	Error of regression

References

1. Lutyński, M.; Kielar, J.; Gajda, D.; Mikeska, M.; Najser, J. High-Pressure Adsorption of CO_2 and CH_4 on Biochar—A Cost-Effective Sorbent for In Situ Applications. *Materials* **2023**, *16*, 1266. [CrossRef]
2. Al-Qadri, A.A.; Nasser, G.A.; Adamu, H.; Muraza, O.; Saleh, T.A. CO_2 utilization in syngas conversion to dimethyl ether and aromatics: Roles and challenges of zeolites-based catalysts. *J. Energy Chem.* **2023**, *79*, 418–449. [CrossRef]
3. Arora, V.; Saran, R.K.; Kumar, R.; Yadav, S. Separation and sequestration of CO_2 in geological formations. *Mater. Sci. Energy Technol.* **2019**, *2*, 647–656. [CrossRef]
4. IPCC. *Climate Change 2023: Synthesis Report*; IPCC: Geneva, Switzerland, 2023. [CrossRef]
5. McLaughlin, H.; Littlefield, A.A.; Menefee, M.; Kinzer, A.; Hull, T.; Sovacool, B.K.; Bazilian, M.D.; Kim, J.; Griffiths, S. Carbon capture utilization and storage in review: Sociotechnical implications for a carbon reliant world. *Renew. Sustain. Energy Rev.* **2023**, *177*, 113215. [CrossRef]
6. Bashir, A.; Ali, M.; Patil, S.; Aljawad, M.S.; Mahmoud, M.; Al-Shehri, D.; Hoteit, H.; Kamal, M.S. Comprehensive review of CO_2 geological storage: Exploring principles, mechanisms, and prospects. *Earth-Sci. Rev.* **2024**, *249*, 104672. [CrossRef]
7. DMRE. *Integrated Resource Plan*; DMRE: Gauteng, Pretoria, South Africa, 2019.
8. Surridge, A.; Kamrajh, N.; Melamane, G.; Mosia, T.; Phakula, D.; Tshivhase, T. CCUS Progress in South Africa. In *Proceedings of the CCUS Progress South Africa, Proceedings of the 15th Greenhouse Gas Control Technologies Conference, Abu Dhabi, United Arab Emirates, 15–18 March 2021*; pp. 15–18. [CrossRef]
9. Yan, J.; Zhang, Z. Carbon Capture, Utilization and Storage (CCUS). *Appl. Energy* **2019**, *235*, 1289–1299. [CrossRef]
10. Chen, S.; Liu, J.; Zhang, Q.; Teng, F.; McLellan, B.C. A critical review on deployment planning and risk analysis of carbon capture, utilization, and storage (CCUS) toward carbon neutrality. *Renew. Sustain. Energy Rev.* **2022**, *167*, 112537. [CrossRef]
11. Ding, Y.; Li, S.; Zhu, B.; Lin, H.; Zhang, J.; Tan, J.; Chen, W. Research on the feasibility of storage and estimation model of storage capacity of CO_2 in fissures of coal mine old goaf. *Int. J. Min. Sci. Technol.* **2023**, *33*, 675–686. [CrossRef]
12. Xu, H.; Sang, S.; Yang, J.; Liu, H. CO_2 storage capacity of anthracite coal in deep burial depth conditions and its potential uncertainty analysis: A case study of the No. 3 coal seam in the Zhengzhuang Block in Qinshui Basin, China. *Geosci. J.* **2021**, *25*, 715–729. [CrossRef]
13. Liu, C.; Sang, S.; Zhang, K.; Song, F.; Wang, H.; Fan, X. Effects of temperature and pressure on pore morphology of different rank coals: Implications for CO_2 geological storage. *J. CO2 Util.* **2019**, *34*, 343–352. [CrossRef]
14. Safaei-Farouji, M.; Misch, D.; Sachsenhofer, R.F. A review of influencing factors and study methods of carbon capture and storage (CCS) potential in coals. *Int. J. Coal Geol.* **2023**, *277*, 104351. [CrossRef]
15. Viljoen, J.; Stapelberg, F.; Cloete, M. *Technical Report on the Geological Storage of Carbon Dioxide in South Africa*; Council for Geoscience: Pretoria, South Africa, 2010.
16. Okolo, G.N.; Everson, R.C.; Neomagus, H.W.J.P.; Sakurovs, R.; Grigore, M.; Bunt, J.R. The carbon dioxide, methane and nitrogen high-pressure sorption properties of South African bituminous coals. *Int. J. Coal Geol.* **2019**, *209*, 40–53. [CrossRef]
17. Mabuza, M.; Premlall, K.; Onyango, M.; Daramola, M.O. Low-high temperature flue gas direct injection in south African bituminous and anthracite coals sorption capacity assessment. *Curr. Sci.* **2018**, *115*, 682–691. [CrossRef]
18. Maphala, T.; Wagner, N.J. Effects of CO_2 storage in coal on coal properties. *Energy Procedia* **2012**, *23*, 426–438. [CrossRef]
19. Premlall, K.; Kipyegon, L. In-situ temperature-depth profile evaluation of South African unmineable coal seams to determine CO_2 sequestration potential. *Can. J. Chem. Eng.* **2023**, *102*, 1381–1394. [CrossRef]
20. Mavhengere, P.; Wagner, N.; Malumbazo, N. Influences of SO_2 contamination in long term supercritical CO_2 treatment on the physical and structural characteristics of the Zululand Basin caprock and reservoir core samples. *J. Pet. Sci. Eng.* **2022**, *215*, 110554. [CrossRef]
21. Okolo, G.N.; Neomagus, H.W.J.P.; Everson, R.C.; Roberts, M.J.; Bunt, J.R.; Sakurovs, R.; Mathews, J.P. Chemical–structural properties of South African bituminous coals: Insights from wide angle XRD–carbon fraction analysis, ATR–FTIR, solid state ^{13}C NMR, and HRTEM techniques. *Fuel* **2015**, *158*, 779–792. [CrossRef]
22. Mabuza, M.; Premlall, K. Alterations in the textural structural properties of coals exposed to flue gas for long-term carbon sequestration. *Carbon Capture Sci. Technol.* **2023**, *7*, 100115. [CrossRef]
23. Liu, S.; Harpalani, S. Evaluation of in situ stress changes with gas depletion of coalbed methane reservoirs. *J. Geophys. Res.: Solid Earth* **2014**, *119*, 6263–6276. [CrossRef]

24. Hou, X.; Liu, S.; Zhu, Y.; Yang, Y. Experimental and theoretical investigation on sorption kinetics and hysteresis of nitrogen, methane, and carbon dioxide in coals. *Fuel* **2020**, *268*, 117349. [CrossRef]
25. Ozdemir, E. Role of pH on CO_2 sequestration in coal seams. *Fuel* **2016**, *172*, 130–138. [CrossRef]
26. Bhebhe, S. The Effect of Coal Composition on Carbon Dioxide Adsorption. *University of the Witwatersrand, Johannesburg*. 2008. Available online: https://wiredspace.wits.ac.za/server/api/core/bitstreams/9889914d-b08b-4f6d-9860-9e150170311e/content (accessed on 22 July 2024).
27. Gertenbach, R.; May. Methane and Carbon Dioxide Sorption Studies on South African Coals. *University of Stellenbosch, Stellenbosch*. 2009. Available online: https://scholar.sun.ac.za/items/8de8c487-a584-4978-a5e3-ced42cf13d1a (accessed on 27 July 2024).
28. Flores, R.M. Chapter 5-Coal Composition and Reservoir Characterization. In *Coal and Coalbed Gas*; Flores, R.M., Ed.; Elsevier: Amsterdam, The Netherlands, 2014; pp. 235–299.
29. Ojeda-López, R.; Domínguez-Ortiz, A.; Felipe, C.; Cervantes-Uribe, A.; Pérez-Hermosillo, I.J.; Esparza-Schulz, J.M. Isosteric Enthalpy Behavior of CO_2 Adsorption on Micro-Mesoporous Materials: Carbon Microfibers (CMFs), SBA-15, and Amine-Functionalized SBA-15. *J. Compos. Sci.* **2021**, *5*, 102. [CrossRef]
30. Ayawei, N.; Ebelegi, A.N.; Wankasi, D. Modelling and Interpretation of Adsorption Isotherms. *J. Chem.* **2017**, *2017*, 3039817. [CrossRef]
31. Erdogan, F.O. Freundlich, Langmuir, Temkin, DR and Harkins-Jura Isotherm Studies on the Adsorption of CO_2 on Various Porous Adsorbents. *Int. J. Chem. React. Eng.* **2019**, *17*, 5. [CrossRef]
32. Kumar, H.; Mishra, M.K.; Mishra, S. Sorption capacity of Indian coal and its variation with rank parameters. *J. Pet. Explor. Prod. Technol.* **2019**, *9*, 2175–2184. [CrossRef]
33. Tambaria, T.N.; Sugai, Y.; Anggara, F. Examination of the Factors Inhibiting CO_2 Adsorption on Coal: A Case Study from Shallow-Depth Low-Rank Coal Seams. *ACS Omega* **2023**, *8*, 42329–42339. [CrossRef]
34. Jasper, E.E.; Ajibola, V.O.; Onwuka, J.C. Nonlinear regression analysis of the sorption of crystal violet and methylene blue from aqueous solutions onto an agro-waste derived activated carbon. *Appl. Water Sci.* **2020**, *10*, 132. [CrossRef]
35. Li, D.; Liu, Q.; Weniger, P.; Gensterblum, Y.; Busch, A.; Krooss, B.M. High-pressure sorption isotherms and sorption kinetics of CH_4 and CO_2 on coals. *Fuel* **2010**, *89*, 569–580. [CrossRef]
36. Di, C.; Wei, Y.; Wang, K.; Deng, P.; Chen, B.; Shen, L.; Chen, Z. The impact of pressurization-induced decrease of capillary pressure and residual saturation on geological carbon dioxide storage. *J. Clean. Prod.* **2025**, *486*, 144573. [CrossRef]
37. Jeong, S.R.; Park, J.H.; Lee, J.H.; Jeon, P.R.; Lee, C.-H. Review of the adsorption equilibria of CO_2, CH_4, and their mixture on coals and shales at high pressures for enhanced CH_4 recovery and CO_2 sequestration. *Fluid Phase Equilibria* **2023**, *564*, 113591. [CrossRef]
38. Foo, K.Y.; Hameed, B.H. Insights into the modeling of adsorption isotherm systems. *Chem. Eng. J.* **2010**, *156*, 2–10. [CrossRef]
39. Nuhnen, A.; Janiak, C. A practical guide to calculate the isosteric heat/enthalpy of adsorption via adsorption isotherms in metal–organic frameworks, MOFs. *Dalton Trans.* **2020**, *49*, 10295–10307. [CrossRef]
40. Schalkwyk, X.; Thovhogi, T. Evaluation of the Coalbed Methane Prospectivity of the Ermelo Coalfield (Amersfoort Project Area), Main Karoo Basin, South Africa. In Proceedings of the Fifth EAGE Eastern Africa Petroleum Geoscience Forum, Online, 30 March–1 April 2021; Volume 1, pp. 1–6. [CrossRef]
41. Bordy, E.M.; Catuneanu, O. Sedimentology of the upper Karoo fluvial strata in the Tuli Basin, South Africa. *J. Afr. Earth Sci.* **2001**, *33*, 605–629. [CrossRef]
42. Mabuza, M.; Premlall, K.; Daramola, M.O. Physicochemical characterization of South African coals upon short-term flue gas exposure using conventional and advanced techniques. *Mater. Sci. Energy Technol.* **2020**, *3*, 25–35. [CrossRef]
43. Mou, P.; Pan, J.; Niu, Q.; Wang, Z.; Li, Y.; Song, D. Coal Pores: Methods, Types, and Characteristics. *Energy Fuels* **2021**, *35*, 7467–7484. [CrossRef]
44. Zhang, J.; Huang, H.; Zhou, W.; Sun, L.; Huang, Z. Study on Pore Structure of Tectonically Deformed Coals by Carbon Dioxide Adsorption and Nitrogen Adsorption Methods. *Energies* **2025**, *18*, 887. [CrossRef]
45. Premlall, K.; Mabuza, M.M.; Potgieter, J.H. Design, construction and performance reliability verification evaluation of a high pressure volumetric sorption system for CO_2 sorption in South African coals. *Pet. Coal* **2019**, *61*, 813–835.
46. Zhao, H.; Bai, Z.; Guo, Z.; Kong, L.; Yuchi, W.; Li, H.; Bai, J.; Li, W. In situ study of the decomposition of pyrite in coal during hydropyrolysis. *J. Anal. Appl. Pyrolysis* **2021**, *154*, 105024. [CrossRef]
47. Dutta, P.; Harpalani, S.; Prusty, B. Modeling of CO_2 sorption on coal. *Fuel* **2008**, *87*, 2023–2036. [CrossRef]
48. Zhang, R.; Liu, S. Experimental and theoretical characterization of methane and CO_2 sorption hysteresis in coals based on Langmuir desorption. *Int. J. Coal Geol.* **2017**, *171*, 49–60. [CrossRef]
49. Haifei, L.; Wenbin, W.; Shugang, L.; Min, Y.; Yang, B. Experimental study on thermodynamics characteristics of CH_4 and CO_2 adsorption on coal. *Saf. Sci. Eng. Technol.* **2018**, *28*, 129–134. [CrossRef]
50. Tsai, S.C.; Juang, K.W. Comparison of linear and nonlinear forms of isotherm models for strontium sorption on a sodium bentonite. *J. Radioanal. Nucl. Chem.* **2000**, *243*, 741–746. [CrossRef]

51. Al-Ghouti, M.A.; Da'ana, D.A. Guidelines for the use and interpretation of adsorption isotherm models: A review. *J. Hazard. Mater.* **2020**, *393*, 122383. [CrossRef]
52. Azizian, S.; Eris, S. Chapter 6-Adsorption isotherms and kinetics. In *Interface Science and Technology*; Ghaedi, M., Ed.; Elsevier: Amsterdam, The Netherlands, 2021; Volume 33, pp. 445–509.
53. Babatunde, K.A.; Negash, B.M.; Jufar, S.R.; Ahmed, T.Y.; Mojid, M.R. Adsorption of gases on heterogeneous shale surfaces: A review. *J. Pet. Sci. Eng.* **2022**, *208*, 109466. [CrossRef]
54. Tóth, J. Uniform interpretation of gas/solid adsorption. *Adv. Colloid Interface Sci.* **1995**, *55*, 1–239. [CrossRef]
55. Serafin, J.; Dziejarski, B. Application of isotherms models and error functions in activated carbon CO_2 sorption processes. *Microporous Mesoporous Mater.* **2023**, *354*, 112513. [CrossRef]
56. Tóth, J. State equation of the solid-gas interface layers. *Acta Chim. Hung.* **1971**, *69*, 311–328.
57. Palodkar, A.V.; Anupam, K.; Roy, Z.; Saha, B.B.; Halder, G.N. High pressure adsorption isotherms of nitrogen onto granular activated carbon for a single bed pressure swing adsorption refrigeration system. *Heat Mass Transf.* **2017**, *53*, 3155–3166. [CrossRef]
58. Chakraborty, A.; Sun, B. An adsorption isotherm equation for multi-types adsorption with thermodynamic correctness. *Appl. Therm. Eng.* **2014**, *72*, 190–199. [CrossRef]
59. Wu, F.-C.; Tseng, R.-L.; Juang, R.-S. Initial behavior of intraparticle diffusion model used in the description of adsorption kinetics. *Chem. Eng. J.* **2009**, *153*, 1–8. [CrossRef]
60. Renaud, O.; Victoria-Feser, M.-P. A robust coefficient of determination for regression. *J. Stat. Plan. Inference* **2010**, *140*, 1852–1862. [CrossRef]
61. Asuero, A.G.; Sayago, A.; González, A.G. The Correlation Coefficient: An Overview. *Crit. Rev. Anal. Chem.* **2006**, *36*, 41–59. [CrossRef]
62. Abdulsalam, J.; Mulopo, J.; Bada, S.O.; Oboirien, B. Equilibria and Isosteric Heat of Adsorption of Methane on Activated Carbons Derived from South African Coal Discards. *ACS Omega* **2020**, *5*, 32530–32539. [CrossRef]
63. Askalany, A.A.; Saha, B.B. Derivation of isosteric heat of adsorption for non-ideal gases. *Int. J. Heat Mass Transf.* **2015**, *89*, 186–192. [CrossRef]
64. Giraldo, L.; Rodriguez-Estupiñán, P.; Moreno-Piraján, J.C. Isosteric Heat: Comparative Study between Clausius–Clapeyron, CSK and Adsorption Calorimetry Methods. *Processes* **2019**, *7*, 203. [CrossRef]
65. Tun, H.; Chen, C.-C. Isosteric heat of adsorption from thermodynamic Langmuir isotherm. *Adsorption* **2021**, *27*, 979–989. [CrossRef]
66. Pan, H.; Ritter, J.A.; Balbuena, P.B. Examination of the Approximations Used in Determining the Isosteric Heat of Adsorption from the Clausius−Clapeyron Equation. *Langmuir* **1998**, *14*, 6323–6327. [CrossRef]
67. Raganati, F.; Alfe, M.; Gargiulo, V.; Chirone, R.; Ammendola, P. Isotherms and thermodynamics of CO_2 adsorption on a novel carbon-magnetite composite sorbent. *Chem. Eng. Res. Des.* **2018**, *134*, 540–552. [CrossRef]
68. Zhou, S.; Wang, H.; Zhang, P.; Guo, W. Investigation of the isosteric heat of adsorption for supercritical methane on shale under high pressure. *Adsorpt. Sci. Technol.* **2019**, *37*, 590–606. [CrossRef]
69. Dutta, P.; Chatterjee, A.; Bhowmik, S. Isotherm characteristics and impact of the governing factors on supercritical CO_2 adsorption properties of coals. *J. CO2 Util.* **2020**, *39*, 101150. [CrossRef]
70. Czerw, K.; Baran, P.; Szczurowski, J.; Zarębska, K. Sorption and Desorption of CO_2 and CH_4 in Vitrinite- and Inertinite-Rich Polish Low-Rank Coal. *Nat. Resour. Res.* **2021**, *30*, 543–556. [CrossRef]
71. Kang, J.; Elsworth, D.; Fu, X.; Liang, S.; Chen, H. Contribution of thermal expansion on gas adsorption to coal sorption-induced swelling. *Chem. Eng. J.* **2022**, *432*, 134427. [CrossRef]
72. Ranathunga, A.S.; Perera, M.S.A.; Ranjith, P.G.; Rathnaweera, T.D.; Zhang, X.G. Effect of Coal Rank on CO_2 Adsorption Induced Coal Matrix Swelling with Different CO_2 Properties and Reservoir Depths. *Energy Fuels* **2017**, *31*, 5297–5305. [CrossRef]
73. Abdulsalam, J.; Mulopo, J.; Bada, S.; Oboirien, B. Natural gas storage properties of adsorbents synthesised from three different coal waste in South Africa. *Fuel* **2020**, *267*, 117157. [CrossRef]
74. Serafin, J.; Dziejarski, B.; Cruz Junior, O.F.; Sreńscek-Nazzal, J. Design of highly microporous activated carbons based on walnut shell biomass for H_2 and CO_2 storage. *Carbon* **2023**, *201*, 633–647. [CrossRef]
75. Masum, S.A.; Sadasivam, S.; Chen, M.; Thomas, H.R. Low Subcritical CO_2 Adsorption–Desorption Behavior of Intact Bituminous Coal Cores Extracted from a Shallow Coal Seam. *Langmuir* **2023**, *39*, 1548–1561. [CrossRef]
76. Murphy, O.P.; Vashishtha, M.; Palanisamy, P.; Kumar, K.V. A Review on the Adsorption Isotherms and Design Calculations for the Optimization of Adsorbent Mass and Contact Time. *ACS Omega* **2023**, *8*, 17407–17430. [CrossRef]
77. Belhachemi, M.; Addoun, F. Comparative adsorption isotherms and modeling of methylene blue onto activated carbons. *Appl. Water Sci.* **2011**, *1*, 111–117. [CrossRef]
78. Dong, Z.; Zhou, J.; Kuang, N.; Zhang, J.; Tian, S.; Xian, X. Enhanced Modeling of CO_2 Adsorption on Shale: Incorporating Volumetric Effects for Accurate Isotherm Predictions. *Energy Fuels* **2025**, *39*, 3188–3202. [CrossRef]

79. Alexander, D.L.J.; Tropsha, A.; Winkler, D.A. Beware of R^2: Simple, Unambiguous Assessment of the Prediction Accuracy of QSAR and QSPR Models. *J. Chem. Inf. Model.* **2015**, *55*, 1316–1322. [CrossRef]
80. Pourhakkak, P.; Taghizadeh, A.; Taghizadeh, M.; Ghaedi, M.; Haghdoust, S. Chapter 1-Fundamentals of adsorption technology. In *Interface Science and Technology*; Ghaedi, M., Ed.; Elsevier: Amsterdam, The Netherlands, 2021; Volume 33, pp. 1–70.
81. Goel, C.; Mohan, S.; Dinesha, P. CO_2 capture by adsorption on biomass-derived activated char: A review. *Sci. Total Environ.* **2021**, *798*, 149296. [CrossRef] [PubMed]
82. Huang, K.; Du, X.; Li, K.; Zhou, J.; Zhang, D.; Abbas, N.; Cheng, Y.; Wu, T.; Liu, G.; He, C. Competitive adsorption of CO_2/CH_4 on coal: Insights from thermodynamics. *Alex. Eng. J.* **2024**, *97*, 114–126. [CrossRef]
83. Skoczylas, N.; Pajdak, A.; Kudasik, M.; Palla Braga, L.T. CH_4 and CO_2 sorption and diffusion carried out in various temperatures on hard coal samples of various degrees of coalification. *J. Nat. Gas Sci. Eng.* **2020**, *81*, 103449. [CrossRef]
84. Siperstein, F.R.; Avendaño, C.; Ortiz, J.J.; Gil-Villegas, A. Analytic expressions for the isosteric heat of adsorption from adsorption isotherm models and two-dimensional SAFT-VR equation of state. *AIChE J.* **2021**, *67*, e17186. [CrossRef]

Disclaimer/Publisher's Note: The statements, opinions and data contained in all publications are solely those of the individual author(s) and contributor(s) and not of MDPI and/or the editor(s). MDPI and/or the editor(s) disclaim responsibility for any injury to people or property resulting from any ideas, methods, instructions or products referred to in the content.